Dry sliding wear, Co-efficient of friction and Corrosion behaviour of Aluminium alloy 2024 Reinforced with Silicon Carbide and Fly ash Hybrid Metal Matrix Composites

[1] M.Mahendra Boopathi , [2] K.P. Arulshri, [3] N. Iyandurai*, and [4]P.Shanmughasundaram
[1]Department of Mechanical Engineering, CMS College of Engineering and Technology, Coimbatore-641 032, TamilNadu, India.
e-mail: boomahe@yahoo.co.in
[2]Department of Mechanical Engineering, KPR Institute of Engineering and Technology, Coimbatore-641 407, TamilNadu, India.
e-mail: kprarulshri@gmail.com
[3]Department of Physics, Thiruvalluvar Govt Arts College, Rasipuram, Namakkal-637 401, TamilNadu, India.
e-mail: ayandurai@rediffmail.com
[4]Department of Automobile Engineering, Karpagam University,Coimbatore-641021. TamilNadu, India.
e-mail: sunramlec@rediffmail.com

***Abstract*-- The present study deals with the investigation relating to dry sliding wear, co-efficient of friction and corrosion behaviour of Al 2024 in the presence of silicon carbide, fly ash and its recipes. Stir casting method have been used to fabricate hybrid metal matrix composites and their wear resistance and co-efficient of friction has been investigated as a function of applied load and sliding distance for a volume fraction of the particles. Pin-on-disc machine was used to assess the wear resistance and co-efficient of friction of the specimens. The volumetric wear loss and co-efficient of friction of pure alloy and composites with sliding distance at a load varied from 15 to 40 N and sliding velocities of 1 m/s and 2 m/s were studied. It was observed that the wear rate and also the coefficient of friction of the composites decreased at higher loads and larger sliding distances. Corrosion characteristics of the influence of the mixtures of SiC and fly ash volume percent on Al 2024 were also experimentally assessed. The corrosion behaviour of the specimens was carried out by both the electrochemical impedance and potentiodynamic polarization techniques as these methods boasting superior quality and high reliability. Finally the wear and corrosion tested samples were examined using scanning electron microscope and analysed.**

***Index Term*-- Aluminium 2024, Hybrid metal matrix composites, Fly ash with SiC.**

1. INTRODUCTION

The increased demand of light weight materials with high specific strength in the aerospace and automotive industries has led to the development and use of Al alloy-based composites. The metal matrix composites (MMCs) are slowly replacing the general light metal alloys such as aluminium alloy in different industrial applications where strength, low mass and energy savings are the most important criteria. The combination of various properties like electrical, mechanical, and even chemical can be achieved by the use of different types of reinforcements, i.e., continuous, discontinuous, short, whiskers, etc., with the MMCs [1].

Hybrid metal matrix composites (HMMCs) are second-generation composites where more than one type, shape, and sizes of reinforcements are used to obtain better properties. Hybrid composites possess better properties compared with single reinforced composites as they combine the advantages of their constituent reinforcements [2]. Aluminium2024/(SiC + fly ash) - HMMC is one of the composites which have many unique properties over Al/SiC - MMC and Al/fly ash - MMCs. All the data for MMC and HMMC are presented here in sequence to compare the variations.

Aluminium alloy 2024 has good machining characteristics, higher strength and fatigue resistance than both 2014 and 2017. It is widely used in aircraft structures, especially wing and fuselage structures under tension. It is also used in high temperature applications such as in automobile engines and in other rotating and reciprocating parts such as piston, drive shafts, brake rotors and in other structural parts which require light weight and high strength materials [3]. Aluminium is also a ubiquitous element and one of the trace elements with moderate toxic effect on living organism [4]. One of the main drawbacks of this material system is that they exhibit poor tribological properties. Hence the desire in the engineering community to develop a new material with greater wear resistance and better tribological properties, without much compromising on the strength to weight ratio led to the development of metal matrix composites [5,6].

Silicon carbide is a compound of silicon and carbon with a chemical formula SiC. Silicon carbide was originally produced by a high temperature electrochemical reaction of sand and carbon. Any acids or alkalis or molten salts up to

800°C do not attack silicon carbide. In air, SiC forms a protective silicon oxide coating at 1200°C and is able to be used up to 1600°C. The high thermal conductivity coupled with low thermal expansion and high strength gives this material exceptional thermal shock resistant qualities. Silicon carbide ceramics with little or no grain boundary impurities maintain their strength to very high temperatures, approaching 1600°C with no strength loss. Chemical purity, resistance to chemical attack at temperature and strength retention at high temperatures has made this material very popular as wafer tray supports and paddles in semiconductor furnaces. It is an excellent abrasive and has been produced and made into grinding wheels and other abrasive products for over one hundred years. Today the material has been developed into a high quality technical grade ceramic with very good mechanical properties. It is used in abrasives, refractories, ceramics and numerous high-performance applications [7].

Fly ash is one of the most inexpensive and low density reinforcement available in large quantities as solid waste by-product during combustion of coal in thermal power plants. Coal Combustion Products (CCP) is produced in coal-fired power stations, which burn either hard or brown coal. Due to the mineral component of coal and combustion technique, Fly Ash (FA) is produced [8]. In the US alone each year over 118 million tons of coal combustion products are produced. In India the stature was about 90 million ton during 1995 and is likely to exceed 140 million tons in 2020. Percentage utilization of fly ash differs between countries between 95% in Belgium and the Netherlands and 3% in India in the 1990s [9]. The utilization of fly ash instead of dumping it as a waste material can be both on economic and environmental grounds [10]. There is already a vast body of information on utilization of Fly Ash (FA) in building/construction, production of aggregates and more recently for agriculture [11].

The challenges and opportunities of aluminium matrix composites have been reported much better to that of its unreinforced counterpart [12]. The addition of reinforcing phase significantly improves the tribological properties of aluminium and its alloy system. The thinking behind the development of hybrid metal matrix composites is to combine the desirable properties of aluminium, silicon carbide and fly ash. Aluminium have useful properties such as high strength, ductility, high thermal and electrical conductivity but have low stiffness whereas silicon carbide and fly ash are stiffer and stronger and have excellent high temperature resistance but they are brittle in nature [13].

In this study, an attempt has been made to fabricate Al 2024/(SiC + fly ash) hybrid metal matrix composites at various proportions. Methods available for the production of hybrid metal matrix composites are powder metallurgy, spray deposition, liquid metal infiltration, squeeze casting, stir casting [14,15]. Though various processing techniques available for particulate or discontinuous reinforced metal matrix composites, stir casting is the technique, which is in use for large quantity commercial production. This technique is most suitable due to its simplicity, flexibility and ease of production for large sized components. Hence stir casting method (also called liquid state method) is used for this study.

The objective of the present work is to form the reinforcing phase within the metallic matrix by reaction of silicon carbide, fly ash and its proportions with aluminium in the metallic melt. To increase the wettability, commercially pure magnesium (1.5%) was added. Dry sliding wear, co-efficient of friction and corrosion behaviour of the specimens were evaluated. The tested specimens were characterized with the help of scanning electron microscope.

2. MATERIALS AND METHODS

2.1. Materials

The matrix material used in the present investigation was commercially pure aluminium alloy 2024. Aluminium was purchased from Perfect Metal Works, Bangaluru, Karnataka, India. Silicon carbide, fly ash and magnesium were commercially available.

2.2. Experimental Work

2.2.1. Sample preparation

The Stir casting method is used for hybrid composite materials fabrication, in which a dispersed phase is mixed with a molten matrix metal by means of mechanical stirring. The liquid composite material is then cast by conventional casting methods and may also be processed by conventional metal forming technologies. For the present study, Al 2024/SiC, Al 2024/ fly ash, and Al 2024/ (fly ash + SiC) hybrid metal matrix composite was prepared by stir casting route. For this we have chosen 100gm of Al 2024 and desired amount of SiC, fly ash, SiC-fly ash mixtures in powder form. Fly ash, SiC and their mixtures were preheated to 300°C for three hours to remove moisture. Aluminium 2024 was melted in a resistance furnace. Then the melt was casted in a clay graphite crucible and it was degassed by purging hexachloro ethane tablets. The melt temperature was raised up to 720°C and then the melt was stirred with the help of a mild steel turbine stirrer. The stirring was maintained between 5 to 7 min at an impeller speed of 200 rpm. To increase the wettability, 1.5% of pure Mg was added with composites. The melt temperature was maintained 700°C during addition of Mg, SiC, fly ash, mixture of SiC-fly ash particles. The dispersion of fly ash and other particles were achieved by the vortex method. The melt with reinforced particulates were poured into the sand casting. The pouring temperature was maintained at 700ºC. The melt was then allowed to solidify in the cast.

2.2.2. Procedure for the Wear Test

A pin- on- disc test apparatus was used to investigate the dry sliding wear characteristics of the Aluminium alloy and its composites as per ASTM G99-95 standards. The wear specimen size of 10 mm× 10 mm and height of 10 mm was cut from cast samples, machined and then polished metallographically. The wear tests were conducted with the load ranging from 15N to 40N at a sliding speed of 1m/s with a constant sliding distance of 1000 metres and a disc rotation speed of rpm 212. All these tests have been conducted in

atmospherics air i.e., at room temperature. The initial weight of the specimen was measured in a single pan electronic weighing machine with a least count of 0.0001 g. During the test, the pin was pressed against the counterpart rotating against EN32 steel disc with hardness 65HRc by applying the load. An approximately strain–gauged friction-detecting arm holds and loads the pin specimen vertically into a rotating hardened steel disc. The frictional traction experienced by the pin during sliding is measured continuously by PC-based data-logging system for post testing analysis. After running through a fixed sliding distance, the specimen were removed, cleaned with acetone, dried and weighed to determine the weight loss due to wear. The difference in the weight measured before and after the test gives the wear of the specimen. The wear rates were determined using the weight loss method. The wear of the composite was studied as a function of the sliding distance, applied load and the sliding velocity. The friction coefficients have been determined from the friction force and normal loads. Samples that we were used to investigate the wear rate and coefficient of friction are presented in Fig.1.

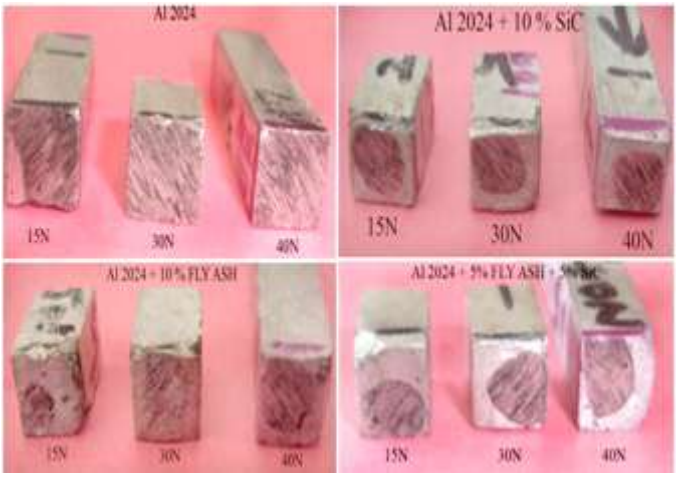

Fig. 1.

2.2.3. Procedure for the Corrosion Test

Corrosion tests for the present study were carried out by Impedance curve interpretation and also the Potentiodynamic Polarization Technique.

Most metal corrosion occurs via electrochemical reactions at the interface between the metal and an electrolyte solution. A thin film of moisture on a metal surface forms the electrolyte for atmospheric corrosion. Wet concrete is the electrolyte for reinforcing rod corrosion in bridges. Although most corrosion takes place in water, corrosion in non-aqueous systems is not unknown.

Corrosion normally occurs at a rate determined by equilibrium between opposing electrochemical reactions. The first is the anodic reaction, in which a metal is oxidized, releasing electrons into the metal. The other is the cathodic reaction, in which a solution species (often O_2 or H^+) is reduced, removing electrons from the metal. When these two reactions are in equilibrium, the flow of electrons from each reaction is balanced, and no net electron flow (electrical current) occurs. The two reactions can take place on one metal or on two dissimilar metals (or metal sites) that are electrically connected.

(i) Impedance curve interpretation

The PARSTAT 2273 is the ultimate potentiostat / galvanostat / FRA, boasting superior quality and high reliability. Its exceptional impedance capability, resolution, speed, high current, and high compliance voltage continues to be the standard against which all other systems are measured. Hence the electrochemical impedance measurements were carried out using a potentiostst / galvanostat / FRA (PARSTAT 2273, Princeton Applied Research, USA). PARASTAT 2273 offers a unique combination of compliance voltage up to ±100V, ±10V scan ranges, and a maximum current of up to ±2A. Data acquisition was performed utilizing the power suite software and analysed using Zsimpwin software (version 3.2.1) which can perform EIS experiments from 1MHz to 10μHz. These measurements can control either potentiostatic (Single Sine, Fast MultiSine, or Mott-Schottky), or galvanostatic, (Galvanostatic EIS) experiments.

A three electrode setup was employed with Platinum (Pt) foil as the auxiliary electrode and saturated Calomel (mercury-mercurous chloride) electrode as the reference electrode. The aluminium composite samples served as the working electrode. Since the samples contained air holes, the composites were immersed in 1.5% NaCl solution for 52 hrs approximately.

Then the composites were tested using a solution of 3.5% NaCl solution. The measurements were carried out in the frequency range of 10^6 - 1 Hz as the open circuit potential by superimposing a sinusoidal AC signal of small amplitude of 10mV after the immersion for 30 mins in the corrosive media. The double layer capacitance (Cdi) and charge transfer (Rct) were obtained from the Nyquist plots. Samples used for corrosion behaviour are shown in Fig. 2

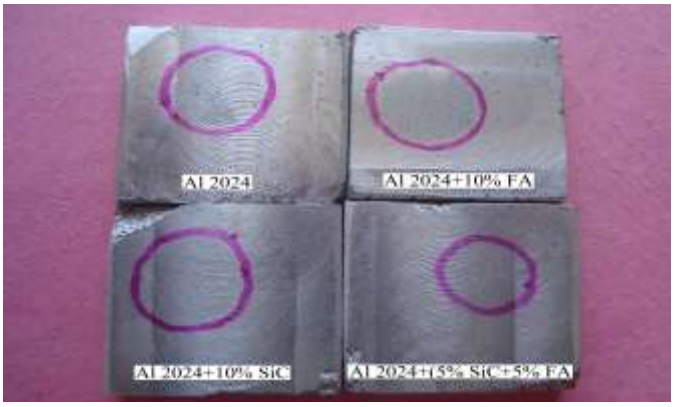

Fig. 2.

(ii) Potentiodynamic Polarization Technique

The potentiodynamic polarization curves (Tafel plots) were measured using the same cell setup employed for the impedance measurements. The potentials were swept at the rate of 1.66mV/sec. Primarily form a mere negative potential Eocp (open circuit potential) to a mere positive potential than Eocp through Ecor (corrosion potential).

Impedance curve is plotted between Zre (real impedance in ohms) and Zim (imaginary impedance in ohms). Potential curve is plotted between log i (current density in Ampere/cm^2)and potential.

2.2.4. Procedure for the Scanning Electron Microscope (SEM)

Microstructural characterization studies were conducted by using scanning electron microscope. The composite samples were metallographically polished prior to examination. Characterization is done in etched conditions. Etching was accomplished using Keller's reagent. The SEM micrographs of composites were obtained using the scanning electron microscope. The images were taken in both secondary electron (SE) and back scattered electron (BSE) mode according to requirement. Microscopic studies to examine the morphology, particle size and micro structure were done by a JEOL 6480 LV scanning electron microscope (SEM) equipped with an energy dispersive X-ray (EDX) detector of Oxford data reference system. Micrographs are taken at suitable accelerating voltages for the best possible resolution using the secondary electron imaging.

3. RESULTS AND DISCUSSION

Wear loss is determined by weight loss technique. The weight loss is converted to volume loss and then wear data is plotted as cumulative volume loss as a function of sliding distance. The wear rate is calculated by using the following formula:

$$W\left(\frac{mm^3}{m}\right)=\frac{\left[\dfrac{M\ (\mathrm{g})}{D\ (\mathrm{g/\,mm^3})}\right]}{Sliding\ Distance\ (\mathrm{m})}$$

where M is the mass loss during wear, and D is the density of the respective composite.

Effect of various parameters on wear volume loss is summarised in Table -1.

Variation of wear volume loss with percentage reinforcement of composites at a sliding speed of 1 m/s and 2 m/s with a load of 40N was also studied (Fig. 3). It was observed that as the percentage of reinforcement increases, the wear of the composites decreases.

The effect of sliding distance on wear volume loss for various composites at a sliding speeds of 1m/sec (Fig. 4) and 2 m/s (Fig. 5) with the load of 40 N were studied. Revolution per minute (rpm) was maintained at 212. It can be seen that as the sliding distance increases from 200 m to 1000 m, the wear of both the composites as well as the unreinforced alloy increases. Noticeably, change in wear is observed even in the initial phase of the sliding distance for composites with different percentages. The incorporation of the mixtures of 5% fly ash and 5% SiC into the Al 2024 alloy improves the sliding wear resistance as compared to the unreinforced alloy. All the observed results confirm that the wear rate is undoubtedly improved in the composites.

The results of the variation of wear volume loss with normal load for various composites at sliding speeds of 1 m/s and 2 m/s with a load of 40 N are shown in Fig. 6 and Fig. 7 respectively. The mild wear is observed at low applied load 15N, as the load increases from 30N to 40N, the wear rate of the unreinforced alloy and the composites increases. Ramesh *et al*. observed the similar results [16].

Table I

Wear in µm (velocity 1 m/s)												
Composition	**Al2024**			**Al2024/10% Flyash**			**Al2024/10% SiC**			**Al2024/5% Flyash+5%SiC**		
Sliding distance(m)	**Load(N)**											
	15	30	40	15	30	40	15	30	40	15	30	40
200	20.22	44.19	64.58	16.87	32.72	48.43	15.86	26.54	46.08	13.94	21.58	36.28
400	37.65	79.58	108.97	32.14	62.99	84.59	29.86	58.22	81.23	25.58	43.58	72.44
600	53.62	109.5	154.04	48.57	96.65	137.24	42.58	85.11	120.22	36.24	71.34	105.58
800	79.65	157.07	234.08	68.65	133.86	198.49	63.87	125.52	180.72	56.87	110.1	163.16
1000	96.24	188.56	290.17	90.74	172.77	252.24	87.58	164.14	245.38	82.59	150.29	220.36

Table II

Wear µm (velocity 2 m/s)												
Composition	**Al2024**			**Al2024/10% Flyash**			**Al2024/10% SiC**			**Al2024/5% Flyash+5%SiC**		
Sliding distance(m)	**Load(N)**											
	15	30	40	15	30	40	15	30	40	15	30	40
200	17.45	44.12	50.34	13.48	32.48	38.9	11.2	21.96	31.39	8.38	14.19	19.48
400	34.65	68.61	102.02	32.15	62.17	88.41	26.8	48.24	69.49	21.28	42.47	49.58
600	48.24	92.12	151.29	41.29	80.51	129.91	39.57	74.19	113.81	31.59	62.73	92.41
800	69.89	138.8	206.81	59.86	118.94	176.03	51.29	100.93	148.37	45.57	88.86	127.07
1000	90.18	177.47	263.89	84.29	164.36	238.4	80.24	158.87	221.12	70.15	142.29	199.6

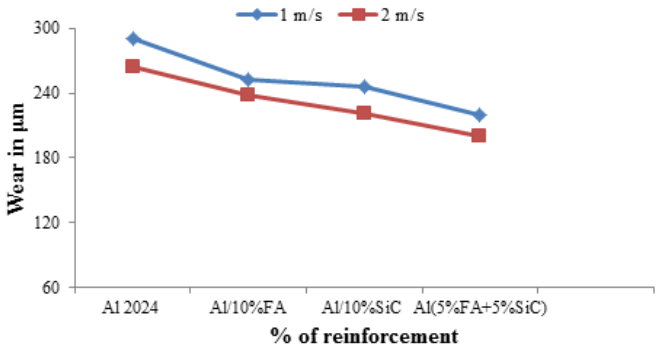

Fig. 3. Variation of wear volume loss with percentage reinforcement of composites at a sliding speed of 1 m/s and 2 m/s with a load of 40N.

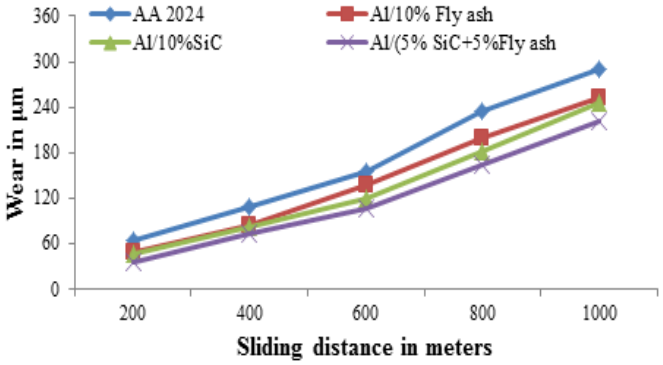

Fig. 3. Variation of wear volume loss with sliding distance for various composites at a sliding speed of 1 m/s and load of 40N.

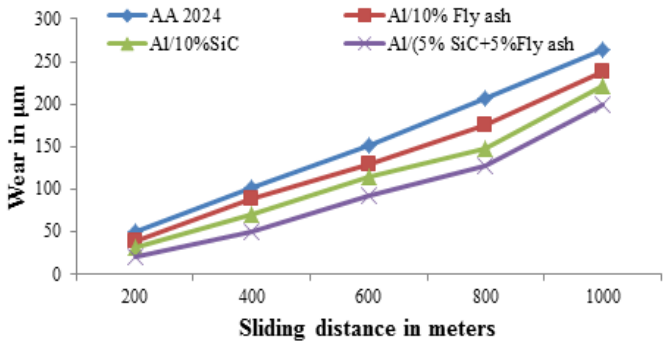

Fig. 4. Variation of wear volume loss with sliding distance for various composites at a sliding speed of 2 m/s and load of 40N.

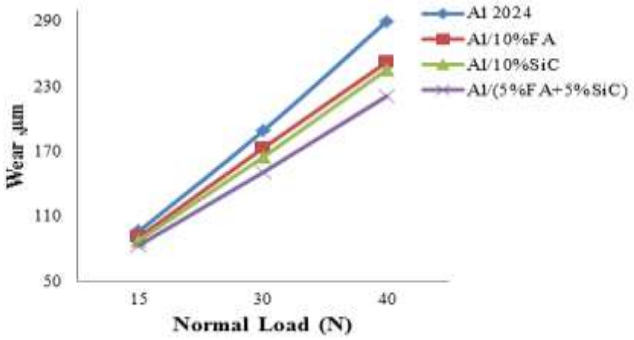

Fig. 5. Variation of wear volume loss with normal load for various composites at a sliding speed of 1 m/s and a sliding distance of 1000 m.

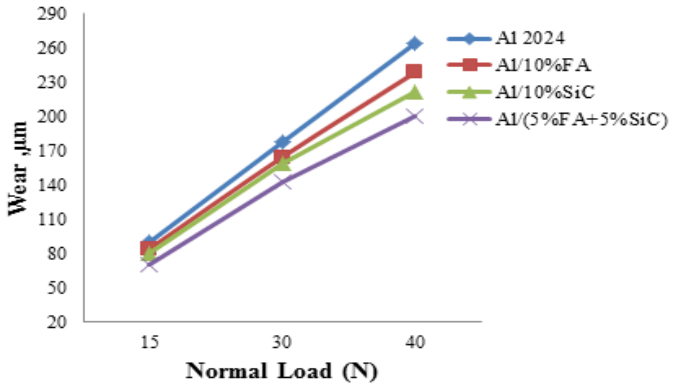

Fig. 6. Variation of wear volume loss with normal load for various composites at a sliding speed of 2 m/s and a sliding distance of 1000 m.

Friction was calculated from the following equation.

$$Kinetic\ Friction\ F_k = \mu_k N$$

$$Kinetic\ Friction\ Coefficient\ \mu_k = \frac{F_k}{N}$$

Where F_k is the kinetic friction, μ_k is the kinetic friction coefficient and N is the normal force.

Effect of various parameters on coefficient of friction is summarised in Table -2.

The effect of sliding distance on coefficient of friction for various composites at sliding speeds of 1m/sec and 2 m/s with the load of 40 N are shown in Fig. 8 and Fig. 9 respectively. It can be seen that as the sliding distance increases from 200 m to 1000 m, the coefficient of friction of both the composites as well as the unreinforced alloy decreases. Change in coefficient of friction is observed even in the initial phase of the sliding distance for composites with different percentages. The incorporation of the mixtures of 5% fly ash and 5% SiC into the Al 2024 alloy improves the coefficient of friction as compared to the unreinforced alloy.

The results of the variation of coefficient of friction with normal load for various composites at sliding speeds of 1 m/s and 2 m/s with a load of 40 N are shown in Fig. 10 and Fig. 11 respectively. The coefficient of friction of Al 2024, Al 2024/10% fly ash and 10% SiC was almost the same at sliding speeds of 1 m/s and 2 m/s. But it was observed that in the presence of 5% flay ash and 5% SiC with Al 2024, the coefficient of friction was considerably decreases. Basavarajappa *et al*. observed the similar results [17]

Table II

Co-efficient of Friction (velocity 1 m/s)

Composition	Al2024			Al2024/10% Flyash			Al2024/10% SiC			Al2024/5% Flyash+5%SiC		
Sliding distance(m)	Load(N)											
	15	30	40	15	30	40	15	30	40	15	30	40
200	0.79	0.77	0.74	0.77	0.75	0.71	0.74	0.73	0.65	0.7	0.71	0.58
400	0.78	0.76	0.74	0.77	0.74	0.7	0.73	0.73	0.65	0.7	0.71	0.58
600	0.77	0.76	0.74	0.76	0.74	0.71	0.73	0.73	0.64	0.69	0.71	0.57
800	0.77	0.76	0.73	0.76	0.74	0.71	0.72	0.72	0.64	0.68	0.7	0.57
1000	0.77	0.75	0.73	0.76	0.73	0.7	0.72	0.72	0.63	0.68	0.7	0.57

Co-efficient of Friction (velocity 2 m/s)

Composition	Al2024			Al2024/10% Flyash			Al2024/10% SiC			Al2024/5% Flyash+5%SiC		
Sliding distance(m)	Load(N)											
	15	30	40	15	30	40	15	30	40	15	30	40
200	0.71	0.68	0.65	0.68	0.67	0.63	0.68	0.66	0.61	0.6	0.57	0.53
400	0.7	0.68	0.64	0.67	0.65	0.63	0.67	0.64	0.6	0.59	0.56	0.52
600	0.69	0.67	0.63	0.67	0.65	0.62	0.66	0.64	0.6	0.58	0.56	0.51
800	0.69	0.66	0.62	0.66	0.64	0.61	0.65	0.63	0.59	0.58	0.55	0.51
1000	0.68	0.66	0.62	0.65	0.64	0.6	0.64	0.62	0.59	0.57	0.54	0.49

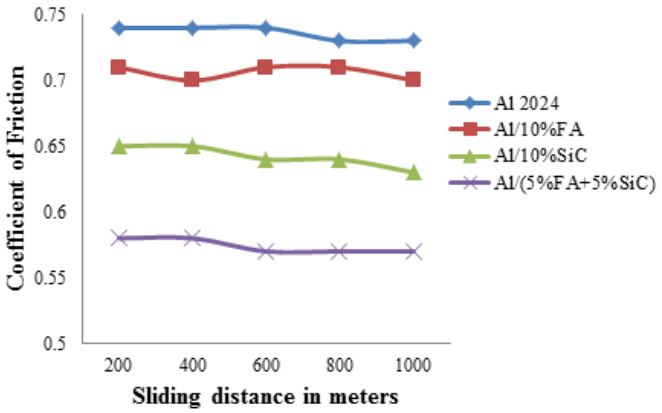

Fig. 8. Variation of coefficient of friction with sliding distance for various composites at a sliding speed of 1 m/s and load of 40N.

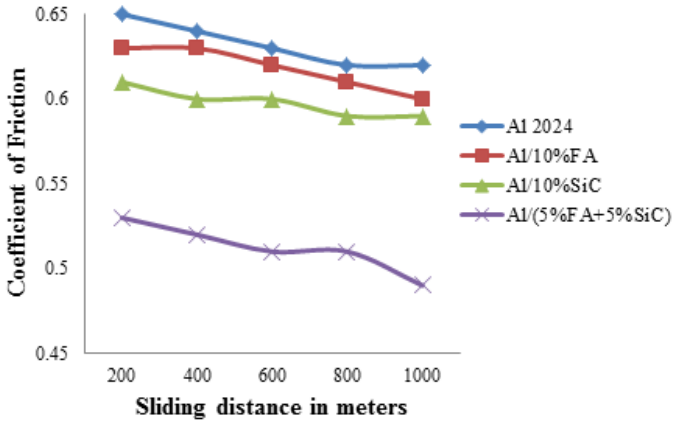

Fig. 9. Variation of coefficient of friction with sliding distance for various composites at a sliding speed of 2 m/s and load of 40N.

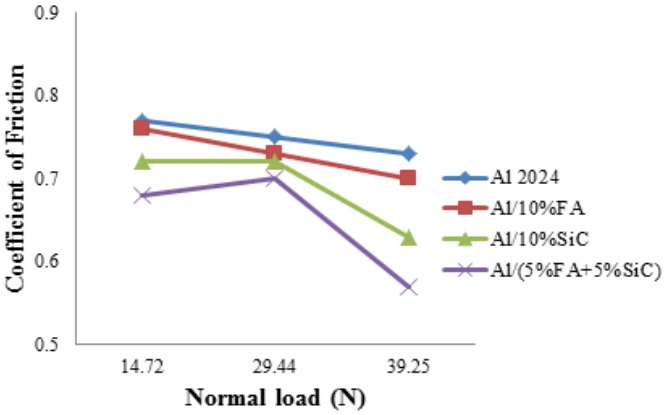

Fig. 10. Variation of coefficient of friction with normal load for various composites at a sliding speed of 1 m/s and a sliding distance of 1000 m.

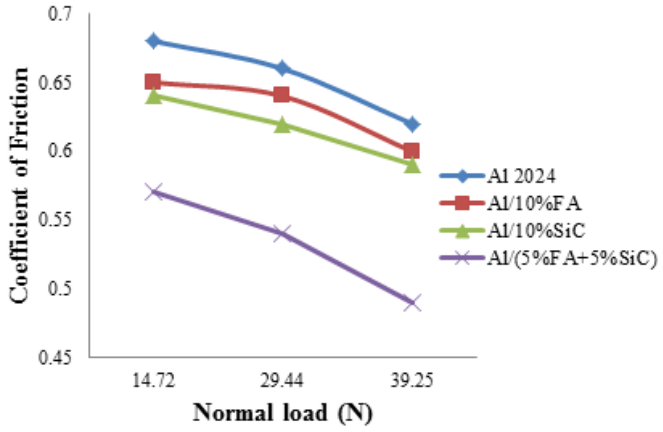

Fig. 11. Variation of coefficient of friction with normal load for various composites at a sliding speed of 2 m/s and a sliding distance of 1000 m.

3.4. Corrosion behaviour

Corrosion protection for Al 2024 and their composites reinforced with various spices of different proportions was investigated. Impedance curve interpretation and Potentiodynamic Polarization Technique were used. The materials studied included Al 2024, Al 2024/10%SiC, Al 2024/10% fly ash and Al 2024/(5%SiC + 5% fly ash).

Corrosion Rate Conversion

The polarization curve of base matrix and composites obtained in 3.5 NaCl sodium chloride solution is shown in Fig. 12. The corrosion potential (E_{corr}) and corrosion current current density (I_{corr}) calculated using Tafel extrapolation method is given in Table III.

Table III

S. No.	Percentage variation of differnt reinceforcements	Corrosion potental, E_{corr} (mVvsSCE)	Corrosion current density, I_{corr} (A/m^2)	Corrosion rate (mm/year)
1	Al 2024	-1.0	0.0002	0.618
2	Al 2024 + 10%SiC	-1.04	0.0004	1.806
3	Al 2024 + 10% fly ash	-1.2	0.0009	2.995
4	Al 2024 + 5%SiC + 5%fly ash	-1.05	0.0006	2.426

In all the cases it is observed that the corrosion rate increases in the begining with increase in test duration and remains constant towards to the end due to passivation. It is clear from the graph that the resistance of the composite to corrosion decreases as the exposure time increases. Similarly, referring the graph that with increase in the weight percentage

of different reinforcement particles the potentail of the different composites with different weight percentage of reinforcement increases. The initial increase in potential is due to the corrosion process which takes place on the surface of the composites. Also, it is clear from the graph that the percentage variation of reinforcements lead to the decrease in current density. For evidence, the addition of fly ash and SiC particles (5% fly ash + 5% SiC) will diminish the corrosion resistance of Al 2024 alloy since that it is difficult to achieve very good bond-ability between ceramic and metal. Mayyas *et al.* observed the similar results [18].

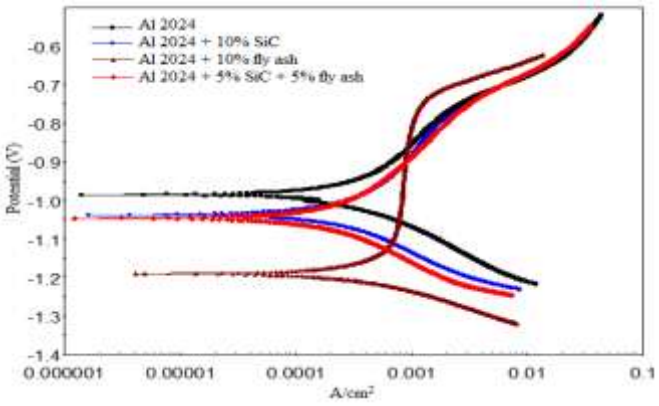

Fig. 12.

The impedance measurement technique has been applied to the study of pitting corrosion and other localized corrosion [19-22]. The impedance technique has marked advantages in the study of interfacial reactions and other interfacial phenomena. The impedance information obtained has time resolved and surface-averaged characteristics [22].

Figure 13 shows the Nyquist plots of the Al 2024 and its composites. Nyquist plot made by plotting the imaginary impedance component (Z_{im}) against the real component (Z_{re}) at each excitation frequency. Frequency is increasing in a counter-clockwise direction. At high frequencies, the impedance is almost entirely created by the solution resistance (R_s). At the low frequencies, the impedance is almost entirely created by the combined polarization resistance (R_p) and solution resistance. Thus, R_p is the difference between the low frequency limit and the high frequency limit. It is apparent that the change in the rotation speed influences the diameter length of the semicircles.

While R_s is the high frequency limiting value of |Z|, the R_p is the difference between the low frequency limit and the high frequency limit. The effect on Rs observed with increasing rotation speed. This behaviour is in agreement with the results which indicate that the corrosion rate increases.

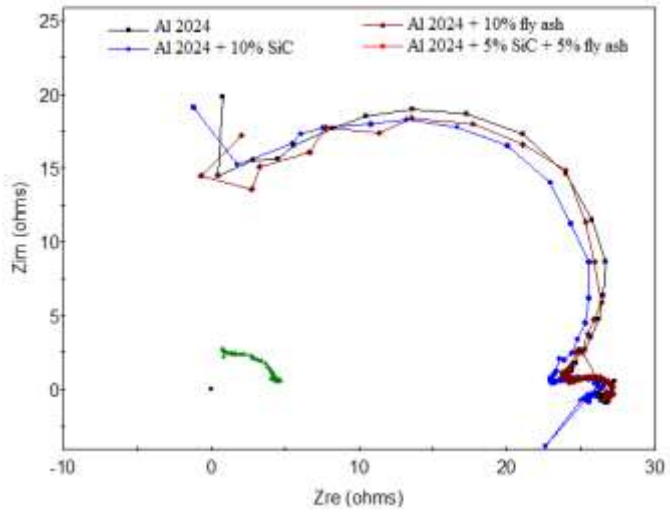

Fig. 13.

3.4. Microstructural Characterization

The worn out surface of some selected /typical specimens after the wear test and corrosion test are observed under scanning electron microscope. Results were compared with earlier studies [23,24].

Scanning electron micrograph of the worn surface of the unreinforced Al 2024 at a speed of 1m/s and a load of 40N after running for a distance of 1000m (after wear) is shown in Fig. 14. The wear surfaces of the unreinforced Al 2024 at a load of 40N consist of two regions long smooth patches and large craters. The long smooth patches consists of ridges and grooves running parallel to the sliding direction which shows an wear was predominant in these regions. The large craters indicate locally adhesive wear. Sliding direction is shown in the Fig.14.

It has been observed that the composites do show improved wear resistance compared to their unreinforced Al 2024. Scanning electron micrograph of the worn surface of the Al 2024/(5%SiC + 5% fly ash) at a speed of 1m/s and a load of 40N after running for a distance of 1000m (after wear) is shown in the Fig. 15. Scanning electron micrograph of worn surface for Al 2024/(5%SiC + 5% fly ash) composite shows the long smooth patches and minimum craters. This indicates typical wear in the composite.

Scanning electron micrograph of the Al 2024 and Al 2024/(5%SiC + 5% fly ash) composites are visualised after subjecting to the corrosion test are shown in Fig. 16 and Fig. 18 respectively. The scanning electron micrographs of corroded samples of matrix and composites reveal more severe pitting and cracks development in unreinforced matrix than in reinforced composites alloy. Greater degree of surface deterioration in composites as observed from SEM images indicates the higher corrosion rates for matrix alloy than for composites. The SEM micrographs show a complete

deterioration of the smoothness of the surface of composites, suggesting the penetration of chloride ions into the material surface forming corrosion spots.

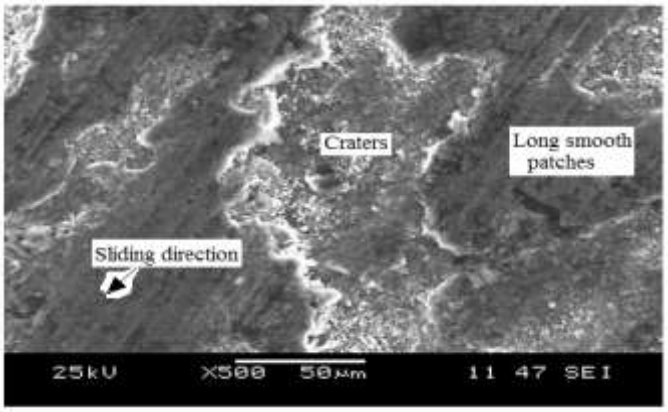

Fig. 14. SEM image of the Al 2024 alloy at a speed of 1m/s and a load of 40N after running for a distance of 1000m (after wear measurement)

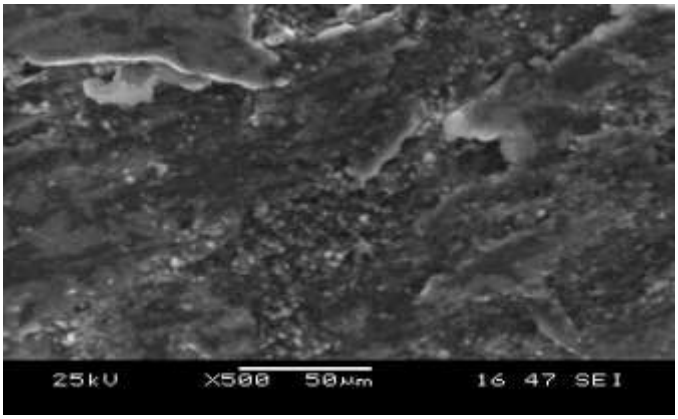

Fig. 15. SEM image of the Al 2024/5%SiC/5%fly ash composite at a speed of 1m/s and a load of 40N after running for a distance of 1000m (after wear measurement)

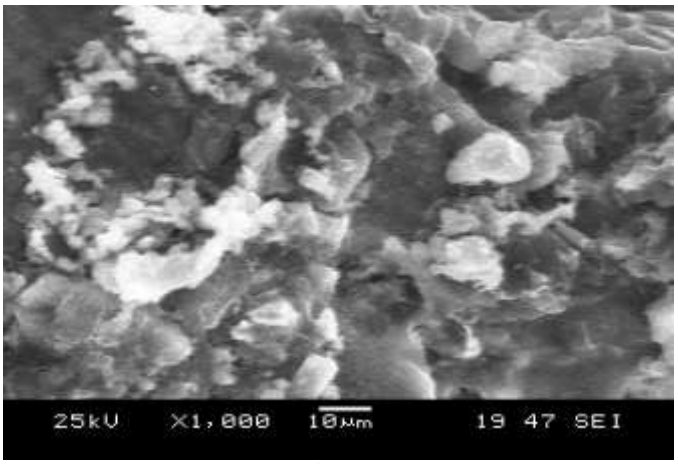

Fig. 16. SEM image of the corroded Al 2024 alloy

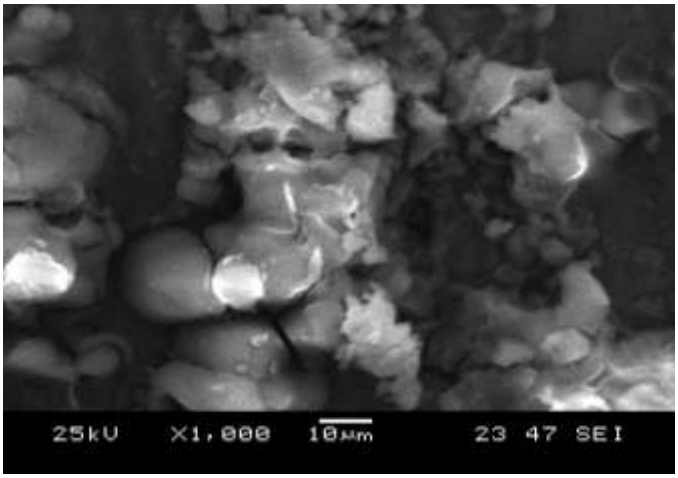

Fig. 17. SEM image of the corroded Al 2024/ (5%SiC/5%fly ash)

4. CONCLUSIONS

Al 2024/10% SiC, Al 2024/10% fly ash, Al 2024/(5% SiC + 5% fly ash) composites were fabricated by stir casting process. Wetting of reinforcements with the aluminium matrix was further improved by the addition of magnesium (1.5%). Based on the experimental observations the following conclusions have been drawn:

- Al 2024/(5% SiC + 5% fly ash) composite exhibit better dry sliding wear resistance than the unreinforced Al 2024 and Al 2024/10% SiC, Al 2024/10% fly ash reinforced composites. This may be due to the work hardening of the surface, formation of iron oxide and the crushing of the SiC and fly ash particles.
- Coefficient of friction varies inversely with the weight fraction of reinforcement and the load. It was observed that the coefficient of friction decreases with increase in the percentage of reinforcements.
- The wear rate also decreases with the increase in the weight percentage of the reinforcements.
- Weight lost is abruptly decreased in the reinforced composites than in unreinforced alloy.
- It was evident that the use of hybrid reinforcement of SiC and fly ash resulted in diminished corrosion resistance of the composites in 3.5% NaCl solution.

REFERENCES

[1] Harish K.Garg, Ketan Verma, Alakesh Manna, Rajesh Kumar, Hybrid Metal Matrix Composites and further improvement in their machinability- A Review, International Journal of Latest Research in Science and Technology, ISSN (Online):2278-5299, Vol.1,Issue 1 :36-44,May-June(2012).

[2] Rajamohan, T., Palanikumar, K., and Ranganathan, S. Evaluation of mechanical and wear properties of hybrid aluminium matrix composites, Trans. Nonferrous Met. Soc. China 23(2013) 2509 -2517.

[3] Ibrahim, I.A., F.A. Mohamed, E.J. Lavernia, 1991. Metal matrix composites-a review. J. Mater. Sci., 26: 1137-1157. DOI: 10.1007/BF00544448

[4] Buraimoh, A.A., S.A. Ojo, J.O. Hambolu and S.S. Adebisi, 2012. Aluminium chloride exposure had no effects on the epididymis of wistar rats. Am. Med. J., 3: 210-219. DOI: 10.3844/amjsp.2012.210.219
[5] Sinclair, I. and P.J. Gregson, 1997. Structural performance of discontinuous metal matrixcomposites. Mater. Sci. Technol., 3: 709-726. DOI: 10.1179/026708397790290254
[6] Sannino, A.P. and H.J. Rack, 1995. Dry sliding wear of discontinuously reinforced aluminum composites: Review and discussion. Wear, 189: 1-19. DOI: 10.1016/0043-1648(95)06657-8
[7] Neudeck, P.G., 1992. An overview of silicon carbide technology. National Aeronautics and Space Administration.
[8] Gatima, E., M. Mwinyihija and K. Killham, 2005. Assessment of Pulverised Fly Ash (PFA) as an ameliorant of lead contaminated soils. Am. J. Environ. Sci., 1: 230-238.
[9] Ulrichs, C., U. Schmidt, T. Mucha-Pelzer, A. Goswami and I. Mewis, 2009. Hard coal fly ash and silicaeffect of fine particulate matter deposits on brassica chinensis. Am. J. Agric. Biol. Sci., 4: 24-31. DOI: 10.3844/ajabssp.2009.24.31
[10] Mohan, S.K.R., K.P. Jayabalan and A. Rajaraman, 2012. Properties of fly ash based coconut fiber composite. Am. J. Eng. Applied Sci., 5: 29-34. DOI: 10.3844/ajeassp.2012.29.34
[11] Brian, R.H., D.B. Hayden and M.A. Powell, 2003. Evaluation of pulverized fuel ash mixed with organic matter to act as a manufactured growth medium. University of Western Ontario.
[12] Surappa, M.K., 2003. Aluminium matrix composites: Challenges and opportunities. Sadhana, 28: 319-334. DOI: 10.1007/BF02717141
[13] Prabu, S.B., L. Karunamoorthy, S. Kathiresan and B. Mohan, 2006. Influence of stirring speed and stirring time on distribution of particles in cast metal matrix composite. J. Mater. Process. Technol., 171: 268- 273. DOI: 10.1016/j.jmatprotec.2005.06.071
[14] Nai, S.M.L. and M. Gupta, 2002. Influence of stirring speed on the synthesis of Al/SiC based functionally gradient materials. Compos. Struct., 57: 227-233. DOI: 10.1016/S0263-8223(02)00089-2
[15] Hashim, J., L. Looney and M.S.J. Hashmi, 1999. Metal matrix composites: Production by the stir casting method. J. Mater. Process. Technol., 92: 1-7. DOI: 10.1016/S0924-0136(99)00118-1
[16] Ramesh, C.S., Anwar Khan, A.R., Ravikumar, N., Savanprabhu, P. (2005), Prediction of wear coefficient of Al6061-TiO_2 Composites, Wear, 259, 602-608.
[17] Basavarajappa, s., Chandramohan, G., Subramanian, R., and Chandrasekar, A. (2006), Materials Science - Poland, 24, No. 2/1, 357-366
[18] Ahmad T. Mayyas, Mohammad M. Hamasha, Abdalla Alrashdan, Adel M. Hassan, Mohammed T. Hayajneh. (2012), Effect of Copper and Silicon Carbide Content on the Corrosion Resistance of Al-Mg Alloys in Acidic and Alkaline Solutions, Journal of Minerals & Materials Characterization & Engineering, 11(4), 335-352.
[19] M. Orado and T. Okl, *Light Metals* 36(1986)416
[20] J. L. Dawson and M. G. S. Ferreira, *Corros. Sci*. 26 (1986)1009
[21] F. Mansfeld and H. Shih, *J. Electrochem. Soc.* 135(1988)1171
[22] P. Q. Zhang, J. X. Wu, W. Q. Zhang, X. Y. Lu and K. Wang, *Corros. Sci*.**,** 34(8)(1993)1343
[23] P. C. R. Nunes and L. V. Ramanathan (*1995*) Corrosion Behavior of Alumina-Aluminum and Silicon Carbide-Aluminum Metal-Matrix Composites. Corrosion: August 1995, Vol. 51, No. 8, pp. 610-617. **doi:** http://dx.doi.org/10.5006/1.3293621
[24] Dobrzanski, L. A., Wlodarczyk, A., Adamiak, M., (2005), Structure, Properties and corrosion resistance of PM Composite materials based on EN AW-2124 aluminium alloy reinforced with the Al2O3 ceramic particles, Journal of Materials Processing Technology, 163-163, 27-32.